We are IntechOpen,
the world's leading publisher of
Open Access books
Built by scientists, for scientists

6,000
Open access books available

148,000
International authors and editors

185M
Downloads

Our authors are among the

154
Countries delivered to

TOP 1%
most cited scientists

12.2%
Contributors from top 500 universities

CLARIVATE ANALYTICS
BOOK CITATION INDEX
INDEXED

WEB OF SCIENCE™

Selection of our books indexed in the Book Citation Index
in Web of Science™ Core Collection (BKCI)

Interested in publishing with us?
Contact book.department@intechopen.com

Numbers displayed above are based on latest data collected.
For more information visit www.intechopen.com

Chapter

Production of Hydrogen via Water Splitting Using Photocatalytic and Photoelectrocatalytic Route

Akhoury Sudhir Kumar Sinha, Umaprasana Ojha,
Zahoor Alam and Ajay Awdheshprasad Tripathi

Abstract

Hydrogen has been intensively explored recently as an energy carrier to meet the growing demand for green energy across the globe. One of the most difficult and significant subjects in hydrogen energy technology is efficiently creating hydrogen from water by utilizing renewable resources such as solar light. Solar-based hydrogen production comprises several routes, namely, photocatalytic, photoelectrocatalytic, and photobiological decomposition. An efficient photocatalyst is desired to accomplish the above objective by utilizing the first two routes with a minimal rate of recombination of photo-generated charge carriers. In this chapter, strategies for preventing recombination of charge carriers in photocatalysts and the development of photocatalysts have been focused on, and its utilization in the procedure for the production of hydrogen via photocatalytic and photoelectrocatalytic processes is described.

Keywords: hydrogen, photocatalysis, charge recombination, water splitting, photoelectrocatalysis

1. Introduction

Rapid urbanization and global warming have been alarming to people across worldwide in the last decade. This has led to the urgency to develop technology for harnessing green energy from renewable energy resources. Regarding this, researchers have been focusing on the production of hydrogen by utilizing solar energy and abundant water resources. Photocatalytic and photoelectrochemical routes have been widely used for the production of hydrogen by utilizing photocatalysts. Semiconductors-based photocatalysts are essential requirements for the photocatalytic process, and an ideal photocatalyst should have a suitable band positioning and band gap for the utilization of solar energy [1, 2]. Oxide-based and chalcogenide-based semiconductors have been developed for the production of hydrogen in both photocatalytic and photoelectrochemical processes [3, 4]. Swift recombination of photoproduced charge carriers, that is, electron and hole in photocatalyst compromise the durability as well as efficiency of utilization of solar radiations. There are various strategies, such as loading of noble metal, enhancement

of crystallinity, morphology variations, coupling semiconductors with others, loading of co-catalysts based on carbonaceous materials, and formation of heterojunction, that have been employed for the prevention of recombination of charge carriers [5, 6].

2. Fundamentals of photocatalysis

Usually, semiconductor materials are used as photocatalysts for the light-induced redox reaction. **Figure 1** illustrates the basic principles of photocatalysis. Semiconductors are characterized by electron structure, namely, valence band (VB) and conduction band (CB). For excitation of charge carrier, when a photon (hv) having energy similar to or higher than the band gap (E_g) of semiconductor falls on the semiconductor, electron migrates from the VB to the conduction band, leaving holes behind. In this excited state, either, electrons of CB and holes in the VB may recombine to dissipate the energy in the form of heat [3].
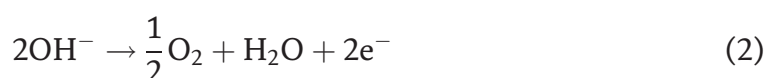
3. Hydrogen production by photocatalytic water dissociation

The dissociation of water comprises two half-reactions, namely, oxidation and reduction of water to oxygen and hydrogen, respectively. The following equations refer to the dissociation of water into oxygen and hydrogen in alkaline media:
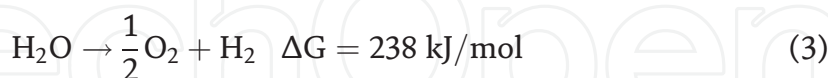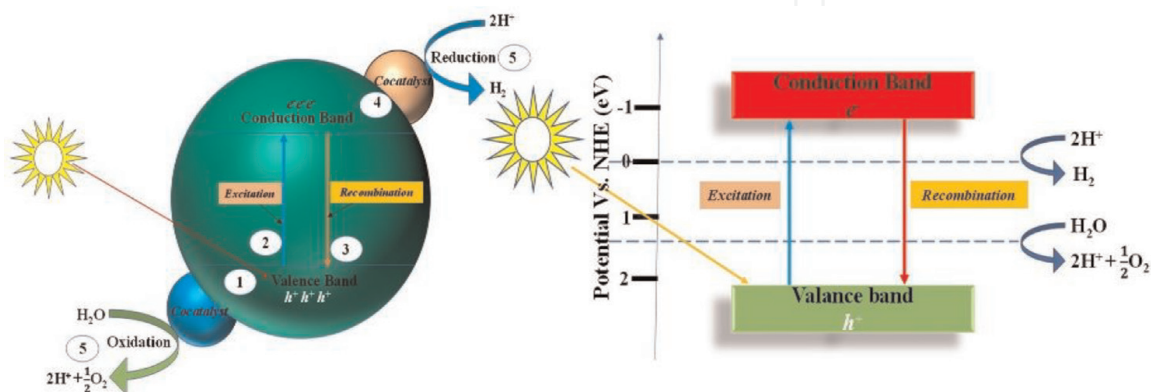
Cathode

$$2H_2O + 2e^- \rightarrow H_2 + 2OH^- \tag{1}$$

Anode

$$2OH^- \rightarrow \frac{1}{2}O_2 + H_2O + 2e^- \tag{2}$$

Overall

$$H_2O \rightarrow \frac{1}{2}O_2 + H_2 \quad \Delta G = 238 \text{ kJ/mol} \tag{3}$$

$$\Delta G = -nFE \tag{4}$$

Figure 1.
*The basic principle of semiconductor-based photocatalysis ref. [3].*

where n stands for the number of electrons associated with the photocatalytic reaction, F is the faraday constant, and E is the redox potential energy of the reaction.

Thermodynamically, the change of Gibbs free energy is positive according to eq. (3); therefore, energy is needed for the dissociation of water. In other words, dissociation of water is not a spontaneous process. The minimum energy required per electron will be 1.13 eV from eq. (4), which is equal to the photon energy of wavelength 1100 nm according to the eq. (5)

$$E = 1240/\lambda \; eV \tag{5}$$

A photon that has an energy of 1.23 eV or greater shall be able to dissociate water. Solar radiation may be utilized as it has a high quantum of photons below the wavelength of 1100 nm. It is important to note that light does not dissociate the water because water is transparent to light. Therefore, a medium (semiconductor catalyst) is required to induce water splitting. A semiconductor has a narrow band gap, where electrons are generated by the utilization of photon of wavelength less than 1100 nm. Moreover, the conduction band gap of catalysts may be preferably more negative than the reduction potential of H_2O to initiate the water-splitting reaction by an electron. Holes at the valence band are used by the sacrificial agents present in the electrolytes.

The overall photocatalytic dissociation of water consists of mainly three steps (as shown in **Figure 2**): (1) electron–hole pair's generation by using the absorption of a photon, (2) electron–hole separation and migration of electrons to the conduction band, (3) reactions between surface species and electron. The first step is photon-physical processes, the second step is the migration of charge carriers, and the third
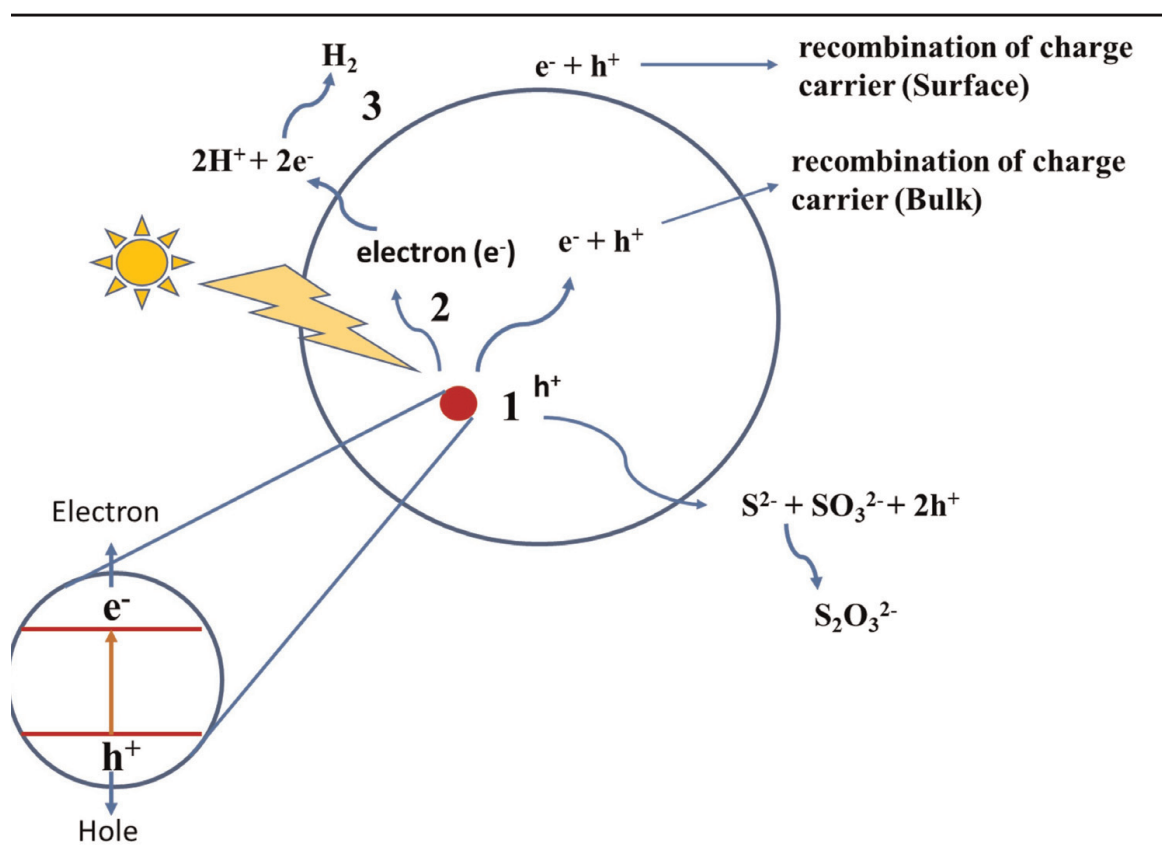
Figure 2.
Fundamental steps associated with the photocatalytic water dissociation of water for hydrogen.

step is the chemical process. Moreover, surface and bulk recombination of electron–hole may also occur. The reverse reaction is also possible in water. Therefore, research is undertaken toward (a) improvement in the harvesting of visible light by utilizing semiconducting materials and (b) efficient charge separation tools and suppressing electron and hole recombination. Apart from these, it is also required to make modifications to the particle morphology of the photocatalyst and adopt the surface structure modification to enhance the rate of the reaction of redox couples.

4. Photoproduced charge recombination phenomenon in photocatalyst

Fast recombination of photoproduced electrons and holes diminishes photocatalytic efficiency, as is well known. The recombination of the photoproduced electron and holes happens in the nanosecond (1×10^{-9} second) range due to a high Coulomb constant (8.99×109 N m^2 C^{2-}) [7]. As a result, preventing the recombination of photoproduced electrons and holes is a more difficult and daunting task. Various tactics for preventing the recombination of photo-induced electron and hole pairs have been proposed in this area, including the loading of noble metals and the coupling of two semiconductors resulting in the creation of a heterojunction at the interface. In general, a heterojunction is a contact between two semiconductors with differing structures. It effectively isolates photo-induced electrons and holes in photocatalysts, increasing photocatalytic efficiency overall.

4.1 Doping of noble metals on the semiconductor surface

For the avoidance of photo-induced electron and hole recombination in semiconductors, loading metal or noble metal on the surface of the semiconductors as co-catalysts has been extensively researched. A Schottky barrier is generated at the interface between the active metal and semiconductors because noble metal has a larger work function than semiconductors. In the literature, the creation of the Schottky barrier has been extensively researched [8]. When noble metals with higher work functions (m) than semiconductors with lower work functions (s) are electrically connected (**Figure 3**), electrons migrate from the conduction band of the semiconductor surface to the active metal until their Fermi levels are aligned, forming a
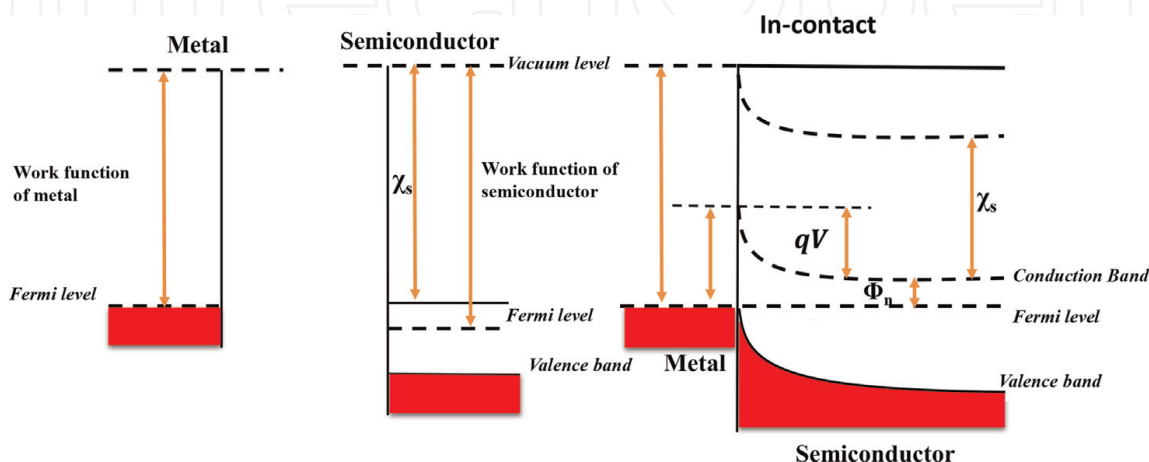
Figure 3.
Energy level diagram of metal surface with n-type semiconductor possessing $\phi_m > \phi_s$ before and after the junction (ref. [9]).

space charge region at the interface between them. As a result, the noble metal will accumulate an excessive amount of negative charge on its surface, whereas the semiconductor will accumulate a positive charge as a result of electron transport. Furthermore, this causes an upward band bending of semiconductors toward the surface. As a result, the Schottky barrier is a tiny barrier that forms in the depleted region.

4.2 Coupling of semiconductors with one another

Making a composite of two or more semiconductors implanted with additional semiconductors with appropriate band energies is another way to boost its photocatalytic activity and stability. According to the literature, a heterojunction formed by the conjunction of two semiconductors can be used to separate charges. Owing to the diffusion of electrons and holes, a p–n junction with a space-charge zone may occur when the p- and n-type semiconductors come into contact (**Figure 4**). As a result, a built-in electrical potential is established, which allows electrons and holes to flow in the opposite direction. Due to the diffusion of electrons and holes, a p–n junction with a space-charge zone may emerge at the interfaces. As a result, a built-in electrical potential is produced, allowing electrons and holes to flow in the opposite direction. The photoproduced electron–hole pairs can be promptly separated by the induced electric field within the space charge area when the p–n heterojunction is irradiated by photons with energy greater than or equal to the photocatalyst's band gap. This p–n heterojunction has several advantages: (a) efficient separation of charge; (b) swift charge migration to the active surface; and (c) sustainable charge carrier life. All of these characteristics impact the photocatalytic performance of the p–n heterojunction [10].

4.3 Creation of heterojunction

As we know that recombination of photoproduced charge carriers in a photocatalytic water-splitting process can be considered a devil to hinder the production of hydrogen at a large scale by utilizing ample solar energy. Prevention of charge recombination is a bit challenging and overwhelming task. Regarding this, the creation of heterojunction between the semiconductors at the interfaces is considered a
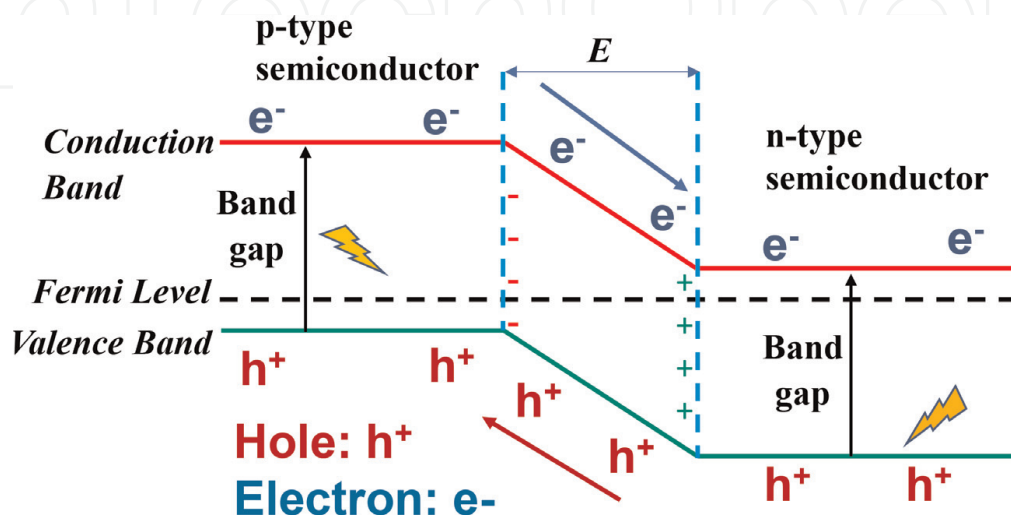

Figure 4.
Schematic representation displaying the band structure and charge carrier separation in the p–n heterojunction ref. [10].

prominent strategy for the designing of efficient photo-catalysts, which could enhance the charge separation efficiency. Low et al. have reported five types of heterojunction in their review literature, namely, convention type-II heterojunction, p-n type heterojunction, surface heterojunction direct Z-scheme heterojunction, and recently developed semiconductor-graphene heterojunctions (SC-Graphene) [9].

5. Advancements in photocatalysts in water splitting

The significant optoelectrical properties, such as electrical conductivity, band gap, and absorption of light, are required for particulate semiconductors-based photocatalytic water splitting. Over four decades, various particulate-based-semi-conductor photocatalysts have been developed, namely, oxide-based photocatalysts (TiO_2, ZnO, $BiVO_4$, $SrTiO_3$, etc.) and chalcogenide-based-photocatalysts (CdS, ZnS, MoS_2, $CdSe$), and are widely used for hydrogen generation based on the photocatalytic water splitting utilizing visible light. However, it has been reported that the fast recombination of photo-induced electrons and holes limits the production of hydrogen at a higher scale. Shao et al. [11] have developed carbonized MoS_2/Mo_2C-decorated CdS with an extraordinary quantum efficiency (41.4% in presence of 420 nm) and reported 112 times greater activity compared to that of the CdS. The exceptional photocatalytic performance of the above system is assigned to the presence of the metallic character of MoS_2 and Mo_2C and an appropriate Gibbs free energy (ΔG) of H_2 adsorption, resulting in increased absorption of photon, rapid separation, and migration of photo-induced carriers, and displaying optimum activity in the HER. Guncai et al. [12] employed the dual-band-gap strategy and prepared CdS-supported reduced graphene oxide (RGO) nano-heterostructure and investigated that interfacial interaction between CdS facilitates the fast transfer of electrons from the CdS to RGO. This interfacial interaction, dependent on the transfer of charge carriers, has been proved theoretically as well as experimentally. Moreover, the transfer of single electron and holes present on the surface of catalysts depends on the surface potential. Surface potential enhances the transfer of electrons to the surface of RGO. Guoning et al. [13] emphasized the stability of heterojunctions between CdS-$Cu_{2-x}S$ and MoS_2 by the migration of ion, that is, Cu, and reported that intercalation of Cu within the MoS_2 basal plane enhances the epitaxial growth of $CuI@MoS_2$ nanosheets in a vertical manner on the surface of 1D core–shell CdS-$Cu_{2x}S$ type nanorods to generate catalytic and protective layers, enhancing catalytic activity and durability at the same time. This design concept shows how hybridized surface layers can be used as efficient catalytic and shielding interfaces for photocatalytic hydrogen generation. Jing et al. [14] fabricated the few-layered MoS_2/$ZnCdS$/ZnS at higher temperatures and constructed the dual heterostructures, which showed a higher rate of production of hydrogen as a result of preventing the recombination of photoproduced electrons and holes. The well-designed structure is effective in the separation and migration of photoproduced electron–hole pairs, leading to an enhancement in photocatalytic H_2 production activity, according to time-resolved photoluminescence spectra. Menglong et al. [15] prepared carbon nitride (CN)-supported red phosphorous (RP) and reported that RP tightly bound with the carbon nitride (CN) framework. A van der Waals heterojunction has been formed between CN and RP and promoted the rapid migration of electrons for the conversion of H^+ ions to H_2 in the process of solar-driven water splitting. Van der

Catalyst	Preparation Method	Light Source	H₂	Ref.
$TiO_2/MoS_2/$ graphene	Hydrothermal MoS_2/graphene Composite prepared. Composite and $Ti(OC_4H_9)$ are reacted hydrothermally to obtain a catalyst	350 W Xe arc lamp	165.3 $\mu mol\ h^{-1}$	[18]
RuDTC: Pt@CdS	CdS nanorods were prepared by seed growth method on it Pt nanoparticle growth was done. Composite of Pt@CdS on its, Ru complex has grown as chemical ligation	$20 mWcm^{-2}$	16 $\mu mol\ h^{-1}$	[19]
CdS Quantum Dots/ZnO	CdS QDs on ZnO (microflowers) by in situ deposition using the SILAR method	225 W xenon arc lamp	22.12 mmol/h*g	[20]
$NiS_{1.97}$	NiO reacts with Thioacetamide in presence of Inter atmosphere (Ar gas)	solar simulator 100 mW/cm^2	~4 $\mu mol\ h^{-1}$	[21]
$La_2Ti_2O_7/CuO$	$La_2Ti_2O_7$ and $Cu(NO_3)_2.3H_2O$ in a crucible for the calcination process.	125 W medium pressure Hg lamp	936.6 mmol h^{-1}	[22]
Se Incorporation in $La_5Ti_2CuS_5O_7$	$La_5Ti_2CuS_5O_7$ and $La_5Ti_2CuS_5O_7$:Se both were prepared by the reaction in a solid state	300 W Xe lamp	~175 $\mu mol\ h^{-1}$	[23]
Palladium Sulfide (PdS)	Pd films in vacuum-sealed ampules with sulfur powder for heating	200 W halogen lamp	~0.55 $\mu mol\ min^{-1}$	[24]
$ZnIn_2S_4$	$Zn(CH_3COO)_2 \cdot 2H_2O$ and thioacetamide hydrothermally give a product	FX-300 Xe lamp	100.1 $\mu mol\ h^{-1}$	[25]
$CdS-Cu_{2-x}S$	Solvothermal or colloidal method CdS and catalyst preparation by a cation exchange process	300 W xenon lamp along with U.V. cut-off filter	14184.8 $\mu mol\ g^{-1}\ h^{-1}$ (20 h)	[13]
$MoS_2/g\ C_3N_4/$ GO	Graphene oxide is prepared by exfoliation MoS_2 by the reported method and g-C_3N_4 too. Composite preparation by anion exchange and hydrothermal.	300 W xenon arc lamp	1.65 $\mu mol\ h^{-1}$	[26]
$CdS/WO_3/$ $CdWO_4$	CdS prepared first and then WO_3 and $CdWO_4$ three of them are reacting to make tricomposite.	Xe lamp	~3100 $\mu mol\ h^{-1}$	[27]
$La_{0.5}Sr_{0.5}Ta_{0.5}$ $Ti_{0.5}O_2N$	Synthesized by nitridation of oxide resulted from a polymerizable complex method	Xe arc lamp (300 W)	18.2 μmol	[28]
$(CuGa)_{0.5}ZnS_2$	$(CuGa)_{0.5}ZnS_2$ synthesis by Vacuum solid-state reaction method	Xe arc lamp (300 W)	25.6 $\mu mol\ h^{-1}$	[29]
$CuGaS_2/RGO$-TiO_2	$CuGaS_2$ composite on RGO-TiO_2	Xe arc lamp (300 W)	6.9 $\mu mol\ h^{-1}$	[30]
Pt/$CuGaS_2$ and RGO-TiO_2	Pt-loaded $CuGaS_2$ composite on RGO-TiO_2	Xe arc lamp (300 W)	19.8 $\mu mol\ h^{-1}$	[30]
$Zn_xCd_{1-x}Se$ Coated with $[Fe(CN)6]^{4-}$	Preparation of the material is via the solid-state method in a quartz ampoule which is sealed	Xe arc lamp (300 W)	0.75 $\mu mol\ h^{-1}$	[31]
CdSe-DF and CdSe-NR (*dendritic fractals and nanorods)	CdSe is prepared by liquid-solid growth mechanism in hydrothermal for the getting different morphologies, on it, Cu_3P is incorporated.	500 W Xe-Hg lamps	46.5 mmol/h/g (CdSe-DF)	[32]

Catalyst	Preparation Method	Light Source	H$_2$	Ref.
CdSe-QD/amp-TiO$_2$	CdO, oleic acid, and trioctylamine were taken in three-necked flasks, degassed under vacuum, simultaneously that Se and trioctylphosphine (TCP) mixture were prepared inside Ar filled glove box. Quickly inject TCP-Se into a three-necked flask at 3000C	AM 1.5 light irradiation	436 μmol/g.h	[33]
ZnIn$_2$S$_4$/MoSe$_2$	ZnIn$_2$S$_4$ prepared in Autoclave. ZnIn$_2$S$_4$/MoSe$_2$ composites prepared by solution-phase hybridization method.	300 W high-pressure Xe arc lamp	2228 μmol/g.h	[34]
MoS$_2$-QDs/g-C$_3$N$_4$	MoS$_2$ quantum dots were prepared by bath and probe sonication. MoS$_2$-QDs/g-C$_3$N$_4$ composite prepared by sonication and after centrifugation	300 W Xe lamp	19.66 μmol h^{-1}	[35]

Table 1.
Photocatalytic activities of various photocatalysts.

walls heterojunction is one of the best types of heterojunction that could increase the efficiency of the photocatalytic H$_2$O splitting route. Kun et al. [16] synthesized CdS supported on the nanosize MoS$_2$–graphene hybrid. They reported that this catalyst showed a significantly higher hydrogen production. They also optimized the quantity of nanosize of MoS$_2$–graphene hybrid and found that the highest photoactivity was observed when 2 wt% of MoS$_2$–graphene was used having MoS$_2$: graphene = 1:2 (mol:mol). The remarkable activity of the prepared photocatalyst was ascribed to the higher rate of absorption of H$^+$ on the unsaturated S atom at the edge of MoS$_2$. It is believed that the presence of graphene could separate the photoproduced electrons and holes and thus retard the recombination of charge carriers. Xiaohu and coworkers [17] also synthesized rGO–CdS by utilizing the hydrothermal procedure using Cd precursor, GO, and Cd(Ac)$_2$.2H$_2$O as a precursor in DMSO. It was sonicated and then this suspension was poured into a stainless-steel autoclave with a Teflon lining for further solvothermal treatment at 453 K. They also prepared rGO–CdS by a precipitation process for comparison. The composite exhibited improved photocatalytic activity toward H$_2$ production compared to that of the CdS, whereas the physical mixtures of rGO and CdS failed to display a similar enhancement in efficacy. The improved activity was assigned due to the incorporation of rGO that promoted suppression of recombination of the photoproduced carrier as an electron-transfer channel and acceptor, as well as a support of CdS in an aqueous solution.

It is well known that heterojunctions, dual-band structure, van der Walls heterojunction, dual heterojunction, and precipitation method could directly influence the activity. These strategies are the advancement in photocatalytic water splitting. The activities of various photocatalysts, preparation methods, and sources of light are reported in **Table 1**.

6. Factors affecting photocatalytic water splitting

Apart from the fabrications and prevention of recombination of photoproduced electrons and holes, various significant factors are also affecting the photoactivity of

photocatalysts such as band gap energy, light intensity, phase of the catalyst, sacrificial agents, and advancement of photoreactor design.

6.1 Band gap

The electronic configuration of semiconductors-based photocatalysts are generally described in term of energy band and can be represented by the difference in energy level by conduction band (CB) and valence band (VB). In general, the acceptor's relative potential level must be less than the semiconductor's CB for thermodynamic reasons. Moreover, a more negative value of the conduction band position is favorable for the reduction of H^+ ions to hydrogen gas (H_2) [36].

6.2 Intensity of light

Concentration of light possessing energy higher than the activation threshold can boost photocatalytic water-splitting efficiency. In terms of UV photon flux, there are two systems for photocatalytic splitting. Chemical processes consume electron–hole pairs quicker than recombination reactions in the first-order regime, which is typical for fluxes from small-scale experiments of 25 mWcm^2. The second-order regime is for greater intensities, where the rate of recombination is normally dominating and has a smaller effect on the reaction rate. Furthermore, the variation of reaction rate in the water-splitting process is considered to be dependent on the wavelength that comes after the photon absorption of the catalyst with a threshold value corresponding to the band gap of the photocatalyst (**Figure 5**) [36].

6.3 Effect of temperature

Thermodynamically, the temperature did not induce the photocatalytic activity because it cannot generate the electron and holes in catalysts. However, the effect of temperature can be generally seen as facilitating the release of the H_2 from the surface
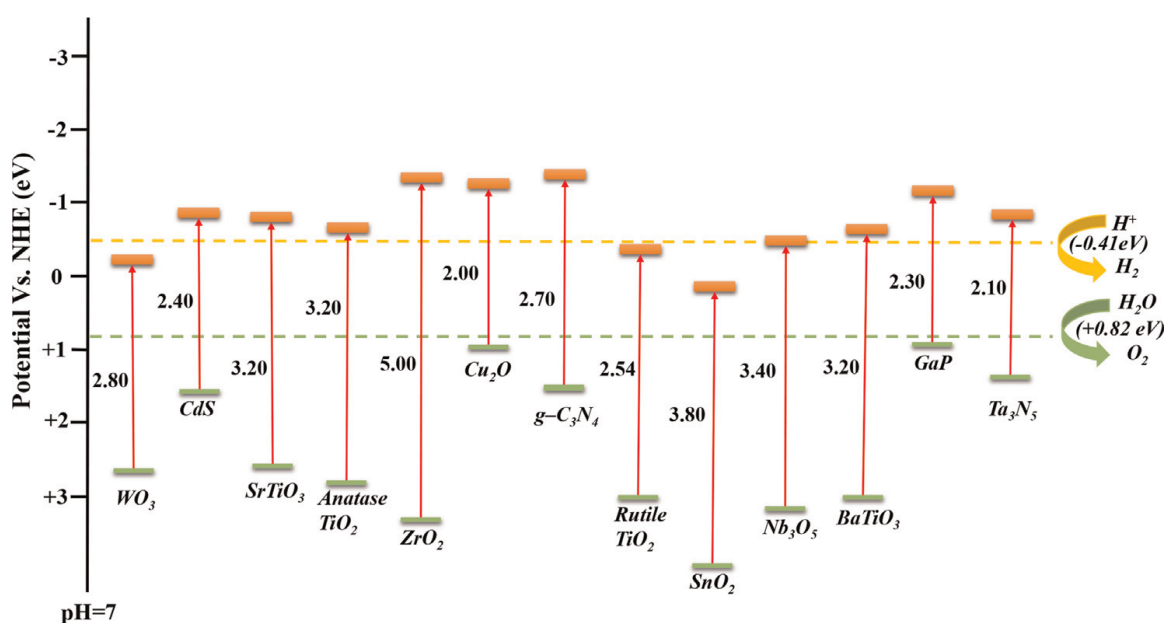

Figure 5.
*Band structure of different types of photocatalysts (ref. [36]).*

of photocatalysts, thus increasing the activity of photocatalytic water splitting. Moreover, the temperature increases the rate of reactions.

6.4 pH

It is well known that the rate of H_2 production from H_2O splitting is dependent on the pH of the solution, that is, hydrogen ions concentration. The hydrogen production is to be generated more effectively in a weak base solution rather than the stronger base solution (pH > 10) or in acidic. Sinha et al. have optimized the pH of the solution (8.6) for a high rate of hydrogen production in the sacrificial agent-mediated photocatalytic reactions [37].

7. Photoelectrochemical water splitting

Photoelectrocatalyst is a material that has the capability of harvesting solar light and chemical transformation by an electrochemical redox reaction. The first photoelectrochemical route for studying water splitting was performed by Fujishima and Honda using TiO_2 catalyst [38, 39]. Photoelectrocatalytic water-splitting reaction is performed in a photoelectrochemical cell. The photoactive material is the semiconductor material that is used for water splitting. In a photoelectrochemical cell setup, which is very similar to an electrochemical cell, either one or both electrodes is photoactive material that is coated on a thin-film-conducting material like ITO/FTO, etc. (**Figure 6**). The photoelectrochemical way of water splitting has an advantage over photocatalytic water splitting, such as the facility of gaseous product separation and external bias voltage that can operate reaction kinetics and mechanism for product choosy. The appealing superiority of photoelectrochemical water splitting takes place at a semiconductor surface, which can generate an electric field at a semiconductor-liquid junction [40]. For the last three decades, the photoelectrochemical route is being used for the generation of hydrogen. Activities of different photoelectrocatalysts are reported in **Table 2**.
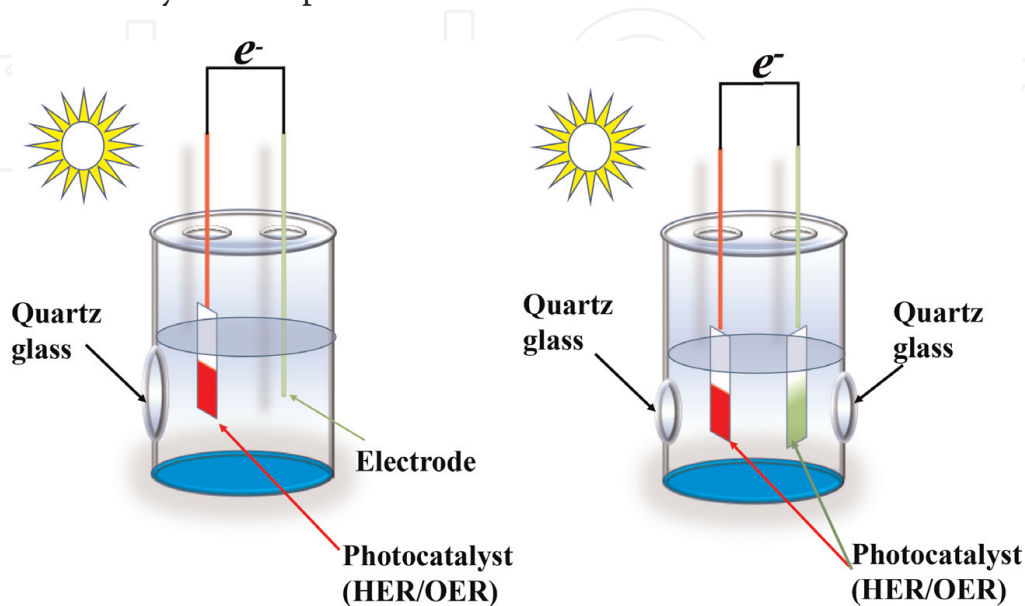
Figure 6.
Schematics of photoelectrochemical cells.

Catalyst	Preparation Method	Light Source	H$_2$	Ref.
n-La$_2$Ti$_2$O$_7$/ p-LaCrO$_3$	La$_2$Ti$_2$O$_7$ is prepared by the calcination process and LaCrO$_3$ is also prepared by the same method as above	125 W medium pressure Hg lamp	267.6 µmol h^{-1}	[41]
Pt-Au/g-C$_3$N$_4$	g-C$_3$N$_4$ is prepared by heating melamine at 5500°C. Pt-Au/gC$_3$N$_4$ is prepared in a Teflon-lined stainless-steel autoclave by putting a solution of Pt and Au salt and gC$_3$N$_4$.	300 W Xe lamp	267.6 µmol .g^{-1}.h^{-1}	[42]
La$_2$Ti$_2$O$_7$/CuO	La$_2$Ti$_2$O$_7$ and Cu(NO$_3$)$_2$.3H$_2$O in a crucible for the calcination process.	125 W medium pressure Hg lamp	936.6 mmol (in 4 h)	[22]
Palladium Sulfide (PdS)	Pd films in vacuum-sealed ampules with sulfur powder for heating	200 W halogen lamp	∼0.55 µmol. Min^{-1}	[24]
ZnIn$_2$S$_4$	Zn(CH$_3$COO)$_2$·2H$_2$O & thioacetamide hydrothermally give a product	FX-300 Xe lamp	100.1 mmol. h^{-1}	[43]
CdS-Cu$_{2-x}$S	Solvothermal or colloidal method CdS and catalyst preparation by a partial cation exchange reaction	300 W xenon (U.V. cut-off filter)	14184.8 µmol. g^{-1}h^{-1} (20 h)	[13]
MoS$_2$/g C$_3$N$_4$/GO	Graphene oxide is prepared by exfoliation MoS$_2$ by the reported method and g-C$_3$N$_4$ too. Composite preparation by anion exchange and hydrothermal.	300 W xenon lamp	1.65 mmol. h^{-1}	[44]
(CuGa)$_{0.5}$ZnS$_2$	(CuGa)$_{0.5}$ZnS$_2$ synthesis by Vacuum solid-state reaction method	300 W Xe lamp	25.6 µmol. h^{-1}	[29]
Zn$_x$Cd$_{1-x}$Se Coated with [Fe(CN)$_6$]$^{4-}$	Preparation of the material is via the solid-state method in a quartz ampoule which is sealed	300 W Xe lamp	0.75 µmol. h^{-1}	[45]
CdSe-QD/ amp-TiO2	CdO, oleic acid, and trioctylamine were taken in three-necked flasks, degassed under vacuum, simultaneously that Se and trioctylphosphine (TCP) mixture were prepared inside Ar filled glove box. Quickly inject TCP-Se into a three-necked flask at 3000°C	AM 1.5 light irradiation	436 µmol/g.h	[46]
ZnIn$_2$S$_4$/MoSe$_2$	ZnIn$_2$S$_4$ preparation in Autoclave which Teflon stainless steel. ZnIn$_2$S$_4$/MoSe$_2$ composites preparation by solution-phase hybridization method.	300 W high-pressure Xe arc lamp	2228 µmol/g^{-1}.h	[34]
CoSx@POP (POP is a porous organic polymer)	7CoSx@POP preparation involves three steps first is POP preparation by oxidative polymerization method second is Co$_3$O$_4$@POP preparation which by heating POP and Co(OAc)$_2$ for 12 hr. in an oil bath and the third step is catalyst preparation	300 W Xenon lamp (420 nm cut-off)	180 µmol/cm^2 after 120 min	[47]
Cu$_2$S-TiO$_2$/TiO$_2$ - NP/FTO	Firstly, a layer of TiO2 grown on FTO glass and, then Cu$_2$S-TiO$_2$ grows on TIO$_2$/FTO	100 W xenon arc-lamp	∼ 55 ± 5 µmol/ cm^{2}hour	[48]
Cu Doped ZnS/ZnO	CuO/ZnO Prepared by solvothermal and catalyst prepared by hydrothermal method	300 W Xe lamp (cut-off filter)	1.044 mmol g^{-1} h^{-1}	[49]

Catalyst	Preparation Method	Light Source	H$_2$	Ref.
g-C$_3$N$_4$/BiVO$_4$	Prepared by hydrothermal for BiVO$_4$ and thermal polycondensation of urea for g-C$_3$N$_4$	500 W halogen lamp	21.4 mmol/h	[50]
Mo-In$_2$O$_3$– ZnIn$_2$Se$_4$	The catalyst prepared by Zn(NO$_3$)$_2$. 6H$_2$O, In(NO$_3$)$_3$·xH$_2$O, and Na$_2$SeO$_3$ by solvothermal reaction	300 W Xe lamp	~1200 µmol/g	[51]

Table 2.
Photoelectrocatalytic activities of various catalysts.

Overall, the following inference can be drawn from the results described in the above section.

- Possibly, chalcogenide based-photocatalysts give higher activities under irradiation of visible light due to the presence of conduction band position toward more negative potential with respect to NHE.

- Reported results show that higher production of hydrogen is seen due to the formation of heterojunction of multiple active catalytic systems.

- Oxide-based photocatalysts have limitation to maximize hydrogen production due to the recombination of photoproduced charge carrier. This may be facilitated by UV light, which comprises ~4–5% of the solar spectrum.

- Results also revealed that the presence of two-dimensional (2D) co-catalysts, such graphene, MoS$_2$, and C$_3$N$_4$ with semiconductors photocatalysts, results in higher activities.

- Nanocatalysts with precise nonmetallic doping may also be helpful to drive the efficiency in a positive direction.

8. Conclusions

Photocatalytic and photoelectrocatalytic routes are considered as sustainable technology for the generation of green and clean hydrogen from renewable sources. Advancements have been made in photocatalysts to prevent the recombination of photoproduced charge carriers, that is, electron and hole. But still both the routes are operational at Research & Development level, and a ground-breaking research is needed in terms of the fabrication of durable and sustainable photocatalysts, development of photoreactor. The catalyst heterostructure, size, shape, and composition controlled the H$_2$ production efficiency under photocatalytic conditions. The availability of photocatalysts with higher efficiency and durability is also desirable for the said purpose. Subsequently, the dispersion of the catalysts in the aqueous medium and their exposure to light during the photocatalysis process is important for large-scale operations. The ability of photocatalysts to produce H$_2$ from low-grade water, wastewater, and sea water is envisaged to further enhance the commercial viability of the process. Other avenues such as photoelectrocatalysis may also be explored to understand the commercial viability of these routes.

Acknowledgements

Conflict of interest

The authors declare no conflict of interest.

Nomenclature

$h\nu$	Energy of photon
VB	Valence band
CB	Conduction band
E_g	Band gap
ΔG	Gibbs free energy
n	Number of electrons
F	Farady constant
λ	Wavelength
N	Newton
m	meter
C	Coulomb
Φ_m	Metalwork function
Φ_s	Semiconductor work function
E_f	Fermi level
ϕ	Work function
s	Electron affinity

Author details

Akhoury Sudhir Kumar Sinha*, Umaprasana Ojha, Zahoor Alam
and Ajay Awdheshprasad Tripathi
Rajiv Gandhi Institute of Petroleum Technology, Jais, Amethi, India

*Address all correspondence to: asksinha@rgipt.ac.in

IntechOpen

References

[1] Sugang M, Jinfeng Z, Shifu C, Sujuan Z, Weixin H. Perspective on construction of heterojunction photocatalysts and the complete utilization of photoproduced charge carriers. Applied Surface Science. 2019; **476**:982-992. DOI: 10.1016/j.apsusc. 2019.01.246

[2] Hui P. Principles on design and fabrication of nanomaterials as photocatalysts for water-splitting. Renewable and Sustainable Energy Reviews. 2016;**57**:584-601. DOI: 10.1016/j.rser.2015.12.117

[3] Xiaobo C, Shaohua S, Liejin G, Samuel SM. Semiconductor-based photocatalytic hydrogen generation. Chemical Reviews. 2010;**110**(11): 6503-6570. DOI: 10.1021/cr1001645

[4] Sha C, Danlian H, Piao X, Wenjing X, Lei L, Min C, et al. Semiconductor-based photocatalysts for photocatalytic and photoelectrochemical water splitting: Will we stop with photocorrosion? Journal of Materials Chemistry A. 2020; **8**:2286-2322. DOI: 10.1039/C9TA12799B

[5] Weiwei H, Lulu C, Weiyu S, Shaobin W, Xiaobin F, Li Y, et al. Synthesis of nitrogen and Sulfur Co-doped reduced graphene oxide as efficient metal-free cocatalyst for the photo-activity enhancement of CdS. Applied Catalysis B: Environmental. 2018;**236**:212-221. DOI: 10.1016/j.ap catb.2018.05.021

[6] Alam Z, Verma B, Sinha ASK. Creation of heterojunction in CdS supported on N, S-rGO for efficient charge separation for photo-reduction of water to hydrogen. International Journal of Hydrogen Energy. 2020;**45**: 4095-4112. DOI: 10.1016/j.ijhydene. 2019.12.056

[7] Jingxiang L, Jiaguo Y, Mietek J, Swelm W, Al-G AA. Heterojunction photocatalysts. Advanced Materials. 2017;**29**:1601694. DOI: 10.1002/adma. 201601694

[8] Amy LL, Guangquan L, John TY, Jr. Photocatalysis on TiO_2 surfaces. Principles, mechanisms, and selected results. Chemical Reviews. 1995;**95**: 735-758. DOI: 10.1021/cr00035a013

[9] Xin L, Rongchen S, Song M, Xiaobo C, Jun X. Graphene-based heterojunction photocatalysts. Applied Surface Science. 2018;**430**:53-107. DOI: 10.1016/j.apsusc.2017.08.194

[10] Huanli W, Lisha Z, Zhigang C, Junqing H, Shijie L, Wan Z. Jianshe Li, and Xinchen W. semiconductor heterojunction photocatalysts: Design, construction, and photocatalytic performances. Chemical Society Reviews. 2014;**43**:5234-5244. DOI: 10.1039/C4CS00126E

[11] Shao M, Yangfan S, Shengjie D, Rui T, Xiongwei Z, Lingmin Y. Weng Fai Ip Baomin X Xing-Qiang S, Yi-Yang S, Xuesen W, and Hui Pan. Carbonized MoS_2: Super-active Co-catalyst for highly efficient water splitting on CdS: ACS sustainable. Chemical Engineer. 2019;7:4220-4229. DOI: 10.1021/acssuschemeng.8b05917

[12] Guancai X, Liming G, Linjuan Z, Beidou G, Aisha B, Qi X, et al. Interaction-dependent interfacial charge-transfer behavior in solar water-splitting system. Nano Letters. 2019;**19**: 1234-1241. DOI: 10.1021/acs. nanolett.8b04768

[13] Guoning L, Charles K, Rong J, Shaopeng Q, Yongbing L, Jinxi C, et al.

MoS$_2$-stratified CdS-Cu$_{2-x}$S Core−Shell nanorods for highly efficient photocatalytic hydrogen production. ACS Nano. 2020;**14**:5468-5479. DOI: 10.1021/acsnano.9b09470

[14] Jing D, Wenjian F, Hui Y, Weiwei X, Xianghua Z, Wenfeng S. Few-layered MoS$_2$/ZnCdS/ZnS heterostructures with an enhanced photocatalytic hydrogen evolution. ACS Applied Energy Materials. 2022;**5**(4):4893-4902. DOI: 10.1021/acsaem.2c00301

[15] Menglong W, Zhixiao Q, Zhidan D, Rui L, Junbo Z, Dongmei M, et al. Red phosphorus/carbon nitride van der Waals heterostructure for photocatalytic pure water splitting under wide-Spectrum light irradiation: ACS sustainable. Chemical Engineer. 2020;**8**: 13459-13466. DOI: 10.1021/ acssuschemeng.0c04372

[16] Kun C, Zongwei M, Tao W, Qing K, Shuxin Q, Jinhua Y. MoS$_2$/graphene cocatalyst for efficient photocatalytic H2 evolution under visible light irradiation. ACS Nano. 2014;**8**:7078-7087. DOI: 10.1021/nn5019945

[17] Zheng P, Qinggang Z, Tianyou P, Xiaohu Z. One-pot synthesis of reduced graphene oxide–cadmium sulfide nanocomposite and its photocatalytic hydrogen production. Physical Chemistry Chemical Physics. 2011;**13**: 21496-21502. DOI: 10.1039/C1CP22059D

[18] Quanjun X, Jiaguo Y, Mietek J. Synergetic effect of MoS$_2$ and graphene as cocatalysts for enhanced photocatalytic H$_2$ production activity of TiO$_2$ nanoparticles. Journal of the American Chemical Society. 2012; **134**(15):6575-6578. DOI: 10.1021/ ja302846n

[19] Wolff CM, Frischmann PD, Schulze M, Bohn BJ, Wein R, Livadas P,

et al. All-in-one visible- light-driven water splitting by combining nanoparticulate and molecular co-catalysts on CdS nanorods. Nature Energy. 2018;**3**:862-869 https://www.na ture.com/articles/s41560-018-0229-6

[20] Ma D, Jian-W S, Yajun Z, Zhaoyang F, Xin J, C N. Highly efficient photocatalyst based on a CdS quantum dots/ZnO nanosheets 0D/2D heterojunction for hydrogen evolution from water splitting. ACS Applied Materials & Interfaces. 2017;**9**: 25377-25386 https://pubs.acs.org/doi/ 10.1021/acsami.7b08407

[21] Reshma B, Sarika K, Golu P, Rohan F, Dushyant K, Satishchandra O. NiS$_{1.97}$: A new efficient water oxidation catalyst for photoelectrochemical hydrogen generation. ACS Applied Materials & Interfaces. 2015;**7**: 20053-20060 https://pubs.acs.org/doi/ 10.1021/acsami.5b05077

[22] Amtul N, Satyabadi M, Parida KM. Heterojunction conception of n-La$_2$Ti$_2$O$_7$/p-CuO in the limelight of photocatalytic formation of hydrogen under visible light. RSC Advances. 2014; **4**:14633-14643 https://pubs.rsc.org/en/c ontent/articlelanding/2014/ra/c3ra 47037g

[23] Swarnava N, Takashi H, Sun S, Masao K, Tsutomu M, Kazunari D. Effects of Se incorporation in La$_5$Ti$_2$CuS$_5$O$_7$ by annealing on physical properties and photocatalytic H$_2$ evolution activity. ACS Applied Materials & Interfaces. 2019;**11**: 5595-5601 https://pubs.acs.org/doi/ 10.1021/acsami.8b02909

[24] Barawi M, Ferrer IJ, Ares JR, Sanchez C. Hydrogen evolution using palladium Sulfide (PdS) Nanocorals as photoanodes in aqueous solution. ACS Applied Materials & Interfaces. 2014;**6**:

20544-20549 https://pubs.acs.org/doi/
10.1021/am5061504

[25] Zhenjiang L, Xuehua W, Wenli T, Alan M, Lina Y. ACS sustainable CoNi bimetal cocatalyst modifying a hierarchical $ZnIn_2S_4$ nanosheet-based microsphere Noble-metal-free photocatalyst for efficient visible-light-driven photocatalytic hydrogen production. Chemical Engineer. 2019;7: 20190-20201 https://pubs.acs.org/doi/10.1021/acssuschemeng. 9b06430

[26] Min W, Peng J, Jiajia L, Yun Z, Xiuxun H, Zhaomin H. Facile synthesis of MoS_2/g-C_3N_4/GO ternary heterojunction with enhanced photocatalytic activity for water splitting. ACS Sustainable Chemistry & Engineering. 2017;5:7878-7886 https://pubs.acs.org/doi/10.1021/acssuschemeng.7b01386

[27] Haruki N, Tsuyoshi O, Seiji K, Morio N. Visible-light overall water splitting by CdS/WO_3/$CdWO_4$ Tricomposite photocatalyst suppressing Photocorrosion. ACS Applied Energy Materials. 2018;1:6730-6735 https://pubs.acs.org/doi/10.1021/acsaem.8b01600

[28] Hiromu K, Ryosuke A, Kosaku K, Akira Y, Masato K, Hideki K. Utilization of perovskite-type oxynitride $La_{0.5}Sr_{0.5}Ta_{0.5}Ti_{0.5}O_2N$ as an O_2-evolving photocatalyst in Z-scheme water splitting. ACS Applied Energy Materials. 2021;4:2056-2060 https://pubs.acs.org/doi/10.1021/acsaem.0c03055

[29] Shunya Y, Akihide I, Yun HN, Rose A, Akihiko K. Z-schematic solar water splitting using fine particles of H2-evolving $(CuGa)_{0.5}ZnS_2$ photocatalyst prepared by a flux method with chloride salts. ACS Applied Energy Materials. 2020;3:5684-5692 https://pubs.acs.org/doi/10.1021/acsaem.0c00661

[30] Katsuya I, Akihide I, Yun HN, Rose A, Akihiko K. Z-schematic water splitting into H_2 and O_2 using metal Sulfide as a hydrogen-evolving photocatalyst and reduced graphene oxide as a solid-state Electron mediator. Journal of the American Chemical Society. 2015;137:604-607 https://pubs.acs.org/doi/10.1021/ja511615s

[31] Yosuke YK, Yui G, Hikaru M, Hiroto I, Hajime S, Ryu A, et al. Z-scheme overall water splitting using ZnxCd1–xSe particles coated with metal cyanoferrates as hydrogen evolution photocatalysts. ACS Catalysis. 2021;11: 8004-8014 https://pubs.acs.org/doi/10.1021/acscatal.1c01187

[32] Parnapalle R, Dinesh KK, Dinesh S, Deepakkumar T, Vempuluru NR, Shankar MV, et al. Temperature-driven morphology control on CdSe nanofractals and its influence over the augmented rate of H_2 evolution: Charge separation via the S-scheme mechanism with incorporated Cu_3P. ACS Applied Energy Materials. 2021;4:13983-13996 https://pubs.acs.org/doi/10.1021/acsaem.1c02790

[33] Sooho L, Kangha L, Whi DK, Seokwon L, Do Joong S, Doh CL. Temperature-driven morphology control on CdSe nanofractals and its influence over the augmented rate of H_2 evolution: Charge separation via the S-scheme mechanism with incorporated Cu_3P. Journal of Physical Chemistry C. 2014; 118:23627-23634 https://pubs.acs.org/doi/10.1021/jp508315m

[34] Deqian Z, Lang X, Wee-J O, Pengyuan W, Hongfei Z, Yuanzhi C, et al. Hierarchical $ZnIn_2S_4$/$MoSe_2$ nanoarchitectures for efficient Noble-metal-free photocatalytic hydrogen evolution under visible light. ChemSusChem. 2017;10:4624 https://chemistryeurope.onlinelibrary.wiley.com/doi/full/10.1002/cssc.201701345

[35] Xixiong J, Xiangqian F, Jianjian T, Ruolin C, Mengli L, Lingxia Z. MoS_2 quantum dot decorated $g-C_3N_4$ composite photocatalyst with enhanced hydrogen evolution performance. RSC Advances. 2016;**6**:52611-52619 https://pubs.rsc.org/en/content/articlelanding/2016/RA/C6RA07060D

[36] Nur F, Muhammad T. A critical review in strategies to improve photocatalytic water splitting towards hydrogen production. International Journal of Hydrogen Energy. 2019;**2**(44): 540-577. DOI: 10.1016/j.ijhydene.2018. 10.200

[37] Arora MK, Sahu N, Upadhyay SN, Sinha AS. Activity of cadmium Sulfide photocatalysts for hydrogen production from water: Role of support. Industrial and Engineering Chemistry Research. 1999;**38**:2659-2665. DOI: 10.1021/ie980400j

[38] John RH, Aarti M, Suljo L. Design principles for efficient and stable water splitting Photoelectrocatalysts. Accounts of Chemical Research. 2021;**54**: 1992-2002 https://pubs.acs.org/doi/10.1021/acs.accounts.1c00072

[39] Fujishima A, Honda K. Electrochemical photolysis of water at a semiconductor electrode. Nature. 1972; **238**:37-38

[40] Hao W, Hui LT, Cui YT, Jason S, Lianzhou W, Rose A, et al. Photocatalytic and photoelectrochemical systems: Similarities and differences. Advanced Materials. 2019;**32**:1904717. Available from: https://onlinelibrary.wiley.com/doi/abs/10.1002/adma.201904717

[41] Amtul N, Kulamani P. $n-La_2Ti_2O_7$/$p-LaCrO_3$: A novel heterojunction-based composite photocatalyst with enhanced photoactivity towards hydrogen production. Journal of Materials

Chemistry A. 2014;**2**:18405-18412 https://pubs.rsc.org/en/content/article landing/2014/ta/c4ta02401j

[42] Kousik B, Moumita C, Santimoy K, Debabrata P. Bimetallic PtAu alloy nanoparticles-integrated $g-C_3N_4$ hybrid as an efficient photocatalyst for water-to-hydrogen conversion. ACS Applied Materials & Interfaces. 2019;**11**:478-488 https://pubs.acs.org/doi/10.1021/acsami.8b121833

[43] Li Z, Wang X, Tian W, Meng A, Yang L. Sustainable CoNi bimetal cocatalyst modifying a hierarchical $ZnIn_2S_4$ nanosheet-based microsphere Noble-metal-free photocatalyst for efficient visible-light-driven photocatalytic hydrogen production. ACS Sustainable Chemistry & Engineering. 2019;**7**:20190-20201 https://pubs.acs.org/doi/10.1021/acssuschemeng.9b06430

[44] Wang M, Peng J, Li J, Zhao Y, Han X, Hao Z. Facile synthesis of MoS_2/$g-C_3N_4$/GO ternary heterojunction with enhanced photocatalytic activity for water. ACS Sustainable Chemistry & Engineering. 2017;**5**:7878-7886 https://pubs.acs.org/doi/10.1021/acssuschemeng.7b01386

[45] Yosuke K, Yui G, Hikaru M, Hiroto I, Hajime S, Ryu A, et al. Z-scheme overall water splitting using $Zn_xCd_{1-x}Se$ particles coated with metal cyanoferrates as hydrogen evolution photocatalyst. ACS Catalysis. 2021;**11**:8004-8014 https://pubs.acs.org/doi/10.1021/acscatal.1c01187

[46] Sooho L, Kangha L, Whi DK, Seokwon DJS, Doh CLJ. Its influence over the augmented rate of H_2 evolution: Charge separation via the S-scheme mechanism with incorporated Cu_3P. Physical Chemistry C. 2014;**118**:

23627-23634 https://pubs.acs.org/doi/
10.1021/jp508315m

[47] Subhash CS, Santimoy K, Indranil M,
Debabrata P, Prof. Dr. J M. Hierarchical
$ZnIn_2S_4/MoSe_2$ nanoarchitectures for
efficient Noble-metal-free photocatalytic
hydrogen evolution under visible light.
Chemistry - A European Journal. 2017;**23**:
14827 https://chemistry-europe.onlinelib
rary.wiley.com/doi/10.1002/chem.
201702561

[48] Singh SV, Gupta U, Biring S,
Mukherjee B, Pal BN. In-situ grown
nanoscale p-n heterojunction of
Cu2S-TiO2 thin film for efficient
photoelectrocatalytic H2 evolution.
Surfaces and Interfaces. 2022;**28**:101660
https://www.sciencedirect.com/science/
article/pii/S246802302100732X?via%
3Dihub

[49] Wei Z, Yuanfu R, Yuying Z,
Anqiang P, Ting Z. In-situ copper doping
with ZnO/ZnS heterostructures to
promote interfacial photocatalysis of
microsized particles. ChemCatChem.
2021;**13**:564 https://chemistryeurope.
onlinelibrary.wiley.com/doi/10.1002/
cctc.202001407

[50] Mohamad FRS, Habib U, Robabeh B,
Norani MM, Suriati S, Ng YH.
Experimental and DFT insights on
microflower $g-C_3N_4/BiVO_4$
photocatalyst for enhanced
photoelectrochemical hydrogen
generation from Lake water. ACS
sustainable. Chemical Engineer. 2020;**8**:
9393-9403 https://pubs.acs.org/doi/
10.1021/acssuschemeng.0c02063

[51] Yuguang C, Peng Z, Li N, Jianping L,
Yong Y, Yelong Z, et al. Ultrathin
visible-light-driven Mo incorporating
$In_2O_3–ZnIn_2Se_4$ Z-scheme nanosheet
photocatalysts. Advanced Materials.
2019;**31**:31. Available from: https://online
library.wiley.com/doi/10.1002/adma.
201807226